BET and XRD studies on the hydroxyapatite and europium doped hydroxyapatite

C.S. CIOBANU[a,b], E. ANDRONESCU[a], D. PREDOI[b*]

[a]University POLITEHNICA of Bucharest, Faculty of Applied Chemistry and Materials Science, Department of Science and Engineering of Oxide Materials and Nanomaterials, 1-7 Polizu Street, P.O. Box 12-134, 011061 Bucharest, Romania
[b]National Institute for Physics of Materials, P.O. Box MG 07, Bucharest, Magurele, Romania,

Europium doped hydroxyapatite (Eu:HAp) nanocristalline powders was synthesized by co-precipitation method by setting the atomic ratio of Eu/[Eu + Ca] at 0% and 2% and [Ca+Eu] /P at 1.67. The structural properties were characterized by X-ray diffraction (XRD). Nitrogen adsorption–desorption isotherms were obtained on different samples using BET method. The X-ray diffraction analysis revealed that hydroxyapatite is the unique crystalline constituent of all the samples, indicating that Eu has been successfully inserted into the HAp lattice. Based on N_2 adsorption–desorption isotherms investigation, the pore size, surface area and pore volume of europium doped hydroxyapatite are 16.57 nm, 115.06 m^2/g and 0.48 cm^3/g.

1. Introduction

Recently, much attention has been attracted by mesoporous materials due to their high surface areas, large and tunable pore size, and large pore volumes, which are crucial for developing new types of catalysts, adsorbents, drug delivery system, and so on [1,2]. Mesostructured materials are materials with pores of 2–50 nm diameter. In the last decade extensive research has been conducted on the synthesis of these materials. Mesostructured materials have been shown to be promising in many fields, in separation science, in optics, as catalysts and as sensors [3], and their use has recently expanded in the biomedical arena, as drug delivery systems [4-6] and in tissue engineering [7-10]. Hydroxyapatite, $Ca_{10}(PO_4)_6(OH)_2$ (denoted as HAp) is a famous bioceramics materials due to its good biocompatibility, excellent ability to form chemical bond with living bone tissue, and suitable osteoconductivity [11-12]. Moreover, HAp with various morphologies and surface properties have also been investigated as drug carriers for the delivery of a variety of pharmaceutical molecules because of its nontoxic and noninflammatory properties [13]. It was first identified as being the mineral component of bone in 1926. Considering the numerous applications of HAp, different morphologies HAp materials in the form of ceramics body [14], nanostructure [15], uniform porous [16] and mesoporous [17] structure have been widely reported. Among them, mesoporous HAp has attracted more attention, thus, design and development on synthesis method becomes a hot issue [17–19].

Being an important emitter in the red region of the visible spectrum, Eu^{3+} ions have been utilized extensively in color television and high efficiency fluorescent lamps [20-21]. Having a relatively simple energy level scheme, hypersensitive transitions and a non-degenerate $_5D^0$ - $_7F^0$ transition, the trivalent europium Eu^{3+} is widely used to probe the crystallographic sites that it occupies in the apatitic matrix. Therefore, Eu^{3+} ions have been widely used as a local structure probe [22–26].

Recently, there have been several papers reporting the synthesis of HAp via several pathways: cationic [27], anionic [28], catanionic [29,30] and non-ionic templating [31]. However, the outcomes (in terms of surface area) are still not quite as desired, since the BET surface areas and pore volumes have been shown to be rather low (<100 m^{2}g^{-1}, <0.3 cm^{3}g^{-1}) [27,30,32,33] as compared with existing mesoporous silica-based materials (1000 m^{2}g^{-1}, 2.0 cm^{3}g^{-1}) [34].

In this paper we describe the synthesis of calcium phosphate ceramics powders doped with Eu^{3+} via coprecipitation method, and the characterizations of these powders by XRD and BET methods.

2. Sample preparation

All the reagents for synthesis including ammonium dihydrogen phosphate [$(NH_4)_2HPO_4$], calcium nitrate [$Ca(NO_3)_2·4H_2O$], and europium nitrate [$Eu(NO_3)_3·6H_2O$] (Alpha Aesare) were used as purchased, without purification.

Europium doped hydroxyapatite (Eu:HAp) nanoparticles was performed by setting the atomic ratio of Eu/[Eu + Ca] at 0% (HAp) and 2% (HAp_E2) and [Ca+Eu] /P at 1.67 [35-38]. The $Eu(NO_3)_3·6H_2O$ and $Ca(NO_3)_2·4H_2O$ were dissolved in deionised water to obtain [Ca+Eu] – containing solution. On the other hand the $(NH_4)_2HPO_4$ was dissolved in deionised water to make P- containing solution. The [Ca+Eu] – containing solution

was put into a Berzelius and stirred at 80°C during 30 minutes. Meanwhile the pH of P- containing solution was adjusted to 10 with NH_3 and stirred continuously for 30 minutes. The P- containing solution was added drop by drop into the [Ca+Eu] – containing solution and stirred for 1h and the pH was constantly adjusted and kept at 10 during the reaction. After the reaction the deposited mixtures were washed several times with deionised water. The resulting material was dried at 100^0C for 50h.

3. Sample characterization

The X-ray diffraction was performed on a Bruker D8 Advance diffractometer, with nickel filtered Cu K_α (λ=1.5418 Å) radiation, and a high efficiency one-dimensional detector (Lynx Eye type) operated in integration mode. The diffraction patterns were collected in the 2θ range 15° – 140°, with a step of 0.02^o and 34 s measuring time per step. In an attempt of performing a complete XRD characterization of the nano-powders, the measured data were processed with the MAUD software, version 2.26 [39].The instrumental line broadening has been evaluated by using a heat treated ceria powder proved to produce no observable size or strain line broadening.

N_2 adsorption/desorption analysis was performed at 77 K using an ASAP 2020 apparatus. The specific surface area was determined by the Bruaauer–Emmett–Teller (BET) method using the data between 0.05 and 0.3. The pore parameters (pore volume and pore diameter) were evaluated from the desorption branch of isotherm based on Barrett–Joyner–Halenda (BJH) model.

4. Results and discussions

4.1 X-ray diffraction

The designed unit formula of Eu doped HAp is: $Ca_{10-x}Eu_x(PO_4)_6(OH)_2$, with x between 0 and 2. The XRD patterns, presented in Figure 1, show the characteristic peaks of hydroxyapatite for each sample, according to ICDD-PDF no. 9-432. No other crystalline phases were detected beside this phase (Figure 1). It can be seen that all samples shows the characteristic peaks of hydroxyapatite structure without secondary phase formation to detect due to doping with Eu^{3+} which demonstrates the complete substitution of Eu^{3+} in hydroxyapatite network.

One can see that doping with the Eu^{3+} cristalinitaty it impacts powders. As the concentration of Eu^{3+} increases 2%, the sample shows a broadening of the lines and a decrease in their intensity suggesting that doping inhibits the growth of particle size of HAp and / or cause network perturbations. XRD spectra of powders obtained were processed using the Maud program.   Thus, after

calculations have obtained results on the network parameters of the samples studied were calculated (Table 1).
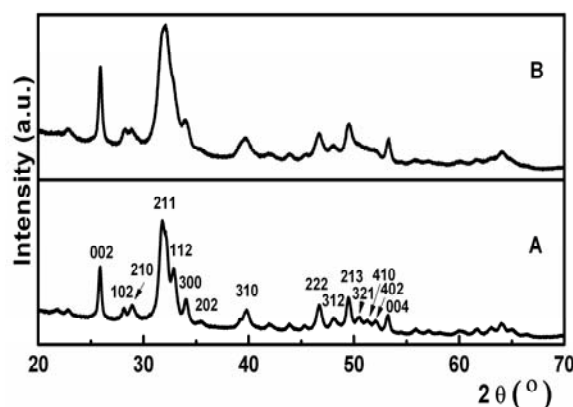

Fig. 1. XRD patterns of the HAp (A) and HAp_E2(B) samples (ICDD-PDF no. 9-432)

Table 1. Network parameters for the HAp and Eu:Hap samples.

Parameters	HAp	HAp_E2
a (Å)	9.4431	9.4386
b (Å)	6.8755	6.8712
D (Å)	207	188

4.2 Adsorption–desorption measurements (BET method)

Porous structure analysis is performed by adsorption - desorption gas analysis. Gas analysis that we use was nitrogen. Nitrogen is easily adsorbed on the surface of solids and its characteristics are well known. The detailed parameters of the pores dispersed on the rod-like HAp grains were determined by N_2 adsorption–desorption isotherms method. Figure 2 shows a typical N_2 adsorption–desorption isotherms for HAp and Eu:Hap samples which exhibit a type IV curve with a hysteresis loop. Type IV isotherms correspond to a mesoporous material. As can be seen from the curves of adsorption and desorption is not a reversible phenomenon which leads to the appearance of a hysteresis between the curves of adsorption and desorption.
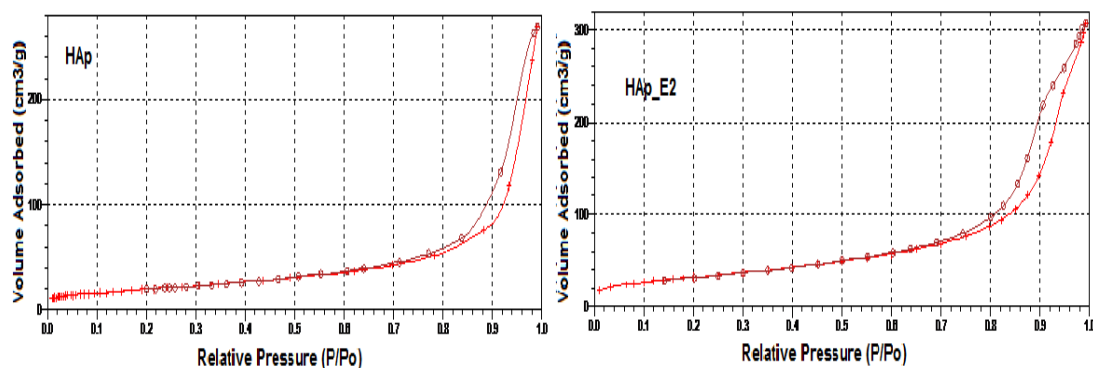
Fig. 2. Typical N_2 adsorption–desorption isotherms for HAP and Eu:Hap samples.

In Fig. 3 present the BET function: $1/[V (P/P_0-1)]$ depending on the P/P_0 for the pure hydroxyapatite (HAp) and europium doped hydroxyapatite (HAp_E2). As is shown BET function was measured in the low pressure of 0.06 and 0.3. Linearity of BET function depending P/P_0 at low pressures show that the application of the BET theory is correct for our samples. The volume of macropores is not very large, because the slope of the adsorption isotherm limited increases in the vicinity $P/P_0 \sim 1$. S_{BET} is reduced by substituting the Eu, as can be seen clearly in Figure 2. A decrease in pore volume for samples Eu-HAp can be also observed.
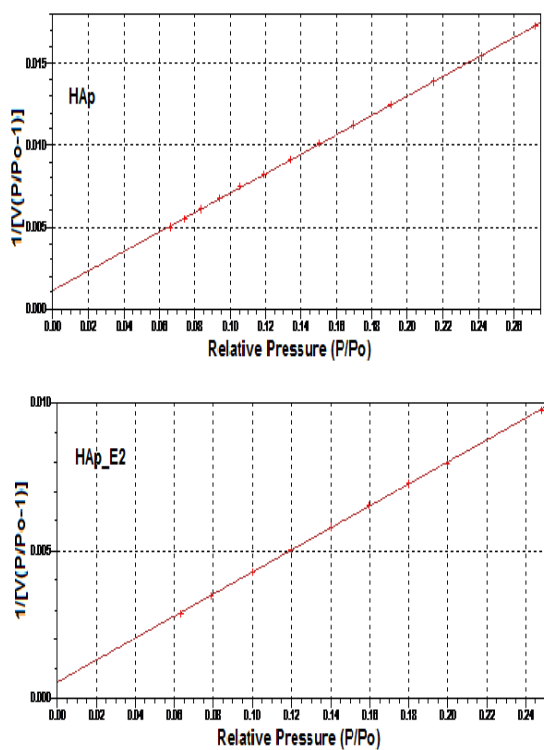
The pore size calculated from the adsorption branch of the isotherms based on BJH model was shown in the Table 2.

Table 2. Specific surface area, pore size, pore volume and micropore volume of the HAp and Eu:HAp samples

Sample		HAp	HAp_E2
Specific Surface Area [m²/g]	BET	67.97	115.06
	Langmuir	112.25	171.26
	BJH Adsorption	91.29	138.91
	BJH Desorption	100.13	149.18
Pore size [nm]	BET Adsorption	22.36	16.57
	BET Desorption	22.60	15.64
	BJH Adsorption	18.23	13.81
	BJH Desorption	16.66	12.83
Pore volum [cm³/g]		0.41	0.48
Micropore volum [cm³/g]		0.005	0.003

5. Conclusions

In this work we propose a simple co-precipitation method for the synthesis of Eu^{3+} doped hydroxyapatite. Structural study of the powders was performed by XRD. Surface area and pore volume of the samples were studied by gas adsorption-desorption measurements (BET method). We have synthesized europium doped hydroxyapatite nanoparticles by co-precipitation method at low temperature with the atomic ratio Eu/(Ca+Eu) = 0% and 2%. The DRX studies have shown that Eu^{3+} has been successfully doped into HAp. The results reveal that the obtained pure HAp and Eu:HAp particles are well assigned to the hexagonal lattice structure of the hydroxyapatite phase.

Analysis of porous structure was achieved by gas adsorption - desorption using BET method. Isotherms of all samples analyzed show a marked hysteresis curve. The curve is a type IV isotherm, which is characteristic to mesoporos materials. Also, for the samples analyzed was

Fig. 3. BET function : $1/[V(P/P_0-1)]$ for the HAp and HAp_E2 samples.

observed that the porous volume shows a decrease with particle size. In the case of Eu-Hap samples pore volume increase indicates changes in their texture as demonstrated by X-ray diffraction.

References

[1] D.M. Antonelli, J.Y. Ying, Angew. Chem. Int. Ed. **35**, 426(1996).
[2] A. Dong, N. Ren, Y. Tang, Y.Wang, Y. Zhang, W. Hua, Z. Gao, J. Am. Chem. Soc. **125**, 4976(2003).
[3] M.G. Kanatzidis, Adv. Mater. **19**, 1165(2007).
[4] M. Vallet-Regí, F. Balas, D. Arcos, Angew Chem. Int. Ed. **46**, 7548(2007).
[5] M. Vallet-Regí, A. Ramila, R.P. del Real, J. Perez-Pariente, Drug Deliv. Syst. Chem. Mater. **13**, 308(2001).
[6] S. Wang, Microporous Mesoporous Mater. **117**, 1 (2009).
[7] A. Lopez-Noriega, D. Arcos, I. Izquierdo-Barba, Y. Sakamoto, O. Terasaki, M. Vallet-Regí, Chem. Mater.**18**, 3137(2006).
[8] I. Izquierdo-Barba, L. Ruiz-González, J.C. Doadrio, J.M. González-Calbet, M. Vallet-Regí, Solid State Sci. **7**, 983(2005).
[9] M. Vallet-Regí, L. Ruiz-Gonzalez, I. Izquierdo-Barba, J.M. Gonzalez-Calbet, J. Mater. Chem., **16**, 26(2006).
[10] M. Vallet-Regí, Chem. Eur. J. **12**, 5934(2006).
[11] K.S. Vecchio, X. Zhang, J.B.Massie,M.Wang, C.W. Kim, Acta Biomater. **3**, 910(2007).
[12] J.M. Gomez-Vega, E. Saiz, A.P. Tomsia, G.W.Marshall, S.J.Marshall, Biomaterials **21**,105(2000).
[13] A. Almirall, G. Larrecq, J. A. A. Delgado, Biomaterials **17**, 3671(2004).
[14] S.V. Dorozhkin, M. Epple, Angew. Chem. Int. Ed. **41**, 3130(2002).
[15] J. Yao,W. Tjandra, Y.Z. Chen, K.C. Tam, J.Ma, B. Soh, J.Mater. Chem. **13**, 3053(2003).
[16] Y.J. Tang, Y.F. Tang, C.T. Lv, Z.H. Zhou, Appl. Surf. Sci. **254**, 5359(2008).
[17] Y.F. Zhao, J. Ma, Micropor. Mesopor. Mater. **87**, 110(2005).
[18] Y.F. Zhao, J. Ma, G.E.B. Tan, Int. J. Nanosci. **5**, 499(2006).
[19] H.L. Wang, L.F. Zhai, Y.H. Li, T.J. Shi, Mater. Res. Bull. **43**, 1607(2008).
[20] R. Ternane, M. Trabelsi-Ayedi, N. Kbir-Ariguib, B. Piriou, J. Lumin. **81**, 165(1999).
[21] A.A. Bol, A. Meijerink, Phys. Rev. B **58**, R15997 (1998).
[22] N. Murase, R. Jagannathan, Y. Kanematsu, Y. Kawasaki, A. Tomita, T. Yazawa, T. Kushida, J. Lumin. **87–89**, 488 (2000).
[23] R. Ternane, G. Panczer, M.T. Cohen-Adad, C. Goutaudier, G. Boulon, N. Kbir-Ariguib, M. Trabelsi-Ayedi, Opt. Mater. **16**, 291(2001).
[24] A. Doat, M. Fanjul, F. Pelle, E. Hollande, A. Lebugle, Biomaterials **24**, 3365(2003).
[25] A. Doat, F. Pelle, A. Lebugle, J. Solid State Chem. **178**, 2354(2005).
[26] A. Doat, F. Pelle, N. Gardant, A. Lebugle, J. Solid State Chem. **177**, 1179 (2004).
[27] J. Yao, W. Tjandra, Y.Z. Chen, K.C. Tam, J. Ma, B. Soh, J. Mater. Chem. 13, 3053 (2003).
[28] S.H. Zhang, Y.J. Wang, K. Wei, X.J. Liu, J.D. Chen, X.D. Wang, Mater. Lett. **61**, 1341 (2007).
[29] B. Prelot, T. Zemb, Mater. Sci. Eng. C **25**, 553(2005).
[30] S.M. Schmidt, J. McDonald, E.T. Pineda, A.M. Verwilst, Y.M. Chen, R. Josephs, et al. Microporous Mesoporous Mater. **94**, 330(2006).
[31] Y.F. Zhao, J. Ma, Microporous Mesoporous Mater. **87**, 110 (2005).
[32] M. Kitamura, C. Ohtsuki, S. Ogata, M. Kamitakahara, M. Tanihara, T. Miyazaki, J. Am. Ceram. Soc. **88**, 822 (2005).
[33] H. Fan, H. Lei, C.Z. Yu, B. Tu, D.Y. Zhao, Mater. Chem. Phys. **103**, 489 (2007).
[34] M. Vallet-Regí, F. Balas, D. Arcos, Angew Chem. Int. Ed. **46**, 7548 (2007).
[35] C.S. Ciobanu, E. Andronescu, B.S. Vasile, C. M. Valsangiacom, R. V. Ghita, D. Predoi, Optoelectron. Adv. Mater-Rapid. Commu. **4**, 1515 (2010).
[36] D. Predoi, R. A. Vatasescxu-Balcan, I. Pasuk, R. Trusca, M. Costache, J. Optoelectron. Adv. Mater. **10**, 2151 (2008).
[37] D. Predoi, R. V. Ghita, F. Ungureanu, C. C. Negrila, R. A. Vatasescu-Balcan, M. Costache, J.Optoelectron. Adv. Mater. **9**, 3827 (2007).
[38] D. Predoi, M. Barsan, E. Andronescu, R. A. Vatasescu-Balcan, M. Costache, J. Optoelectron. Adv. Mater. **9**, 3609 (2007).
[39] L. Lutterotti, Nuclear Inst and Methods in Physics Research B. **268**, 334 (2010).

_____
*Corresponding author: dpredoi68@gmail.com